Commun Nonlinear Sci Numer Simulat 16 (2011) 3559–3577

Contents lists available at ScienceDirect

Commun Nonlinear Sci Numer Simulat

journal homepage: www.elsevier.com/locate/cnsns

Influence of induced magnetic field and heat transfer on peristaltic transport of a Carreau fluid

T. Hayat [a,b,*], Najma Saleem [a], S. Asghar [b,c], Mohammed Shabab Alhothuali [b], Adnan Alhomaidan [b]

[a] Department of Mathematics, Quaid-i-Azam University, Islamabad 44000, Pakistan
[b] Department of Mathematics, Faculty of Science, King Abdul Aziz University, P.O. Box 80203, Jeddah 21589, Saudi Arabia
[c] Department of Mathematics, CIIT Islamabad, H-8, Islamabad, Pakistan

ARTICLE INFO

Article history:
Received 19 December 2009
Received in revised form 23 December 2010
Accepted 31 December 2010
Available online 18 January 2011

Keywords:
Carreau fluid
Induced magnetic field
Heat transfer

ABSTRACT

The effect of an induced magnetic field on peristaltic flow of an incompressible Carreau fluid in an asymmetric channel is analyzed. Perturbation solution to equations under long wavelength approximation is derived in terms of small Weissenberg number. Expressions have been constructed for the stream function, the axial induced magnetic field, the magnetic force function, the current density distribution and the temperature. Trapping phenomenon is examined with respect to emerging parameters of interest.

1. Introduction

The peristalsis comes from a Greek word peristaltikos which means compressing and clasping. Hence peristalsis is a process by which transport of fluid occurs through a distensible tube when progressive waves of area contraction and expansion propagate along its length. Such process is very common in physiology and industry. The biomedical instruments, for instance the blood pumps in dialysis and the heart lung machine involve the mechanism of peristalsis. In order to avoid contamination of the outside environment, the process of peristaltic transport of a toxic liquid in nuclear industry is quite useful.

Since pioneering works of Latham [1] and Shapiro et al. [2], the peristaltic motion has been extensively studied in both mechanical and physiological situations under different conditions. Mention can be made to some interesting recent studies [3–15] in this direction. However, the interaction of peristalsis in presence of an induced magnetic field and heat transfer has not been accorded much attention. Concept of heat transfer analysis is very useful in accessing the blood flow rate through the initial thermal conditions and the thermal clearance rate. The flow of blood can be estimated by a dilation technique. In this process, heat is either injected or generated locally and the thermal clearance is monitored. Specifically the bioheat transfer plays a vital role in destroying undesirable tissues, hyperthermia, laser therapy and cryosurgery [3]. Recently, Mekheimer [16,17] examined the peristaltic transport of couple stress and micropolar fluids under the influence of an induced magnetic field. Hayat et al. [18] have discussed the induced magnetic field effects on peristaltic flow of a third order fluid in symmetric channel.

In this communication, the interaction of peristalsis with an induced magnetic field and heat transfer has been studied for the motion of a Carreau fluid in an asymmetric channel. The flow modeling is based upon the constitutive, continuity, momentum, energy, Maxwells' and induction equations. Series solutions are presented. Variation of pertinent parameters on the flow quantities are sketched and discussed.

* Corresponding author at: Department of Mathematics, Quaid-i-Azam University, Islamabad 44000, Pakistan.
E-mail address: pensy_t@yahoo.com (T. Hayat).

1007-5704/$ - see front matter © 2011 Elsevier B.V. All rights reserved.
doi:10.1016/j.cnsns.2010.12.038

2. Development of the mathematical problem

Let us investigate the MHD flow of an incompressible Carreau fluid in an asymmetric channel of width $d_1 + d_2$. The sinusoidal waves traveling down its walls are written as follows:

$$Y = h_1'(X,Y,t) = d_1 + a_1\cos\left[\frac{2\pi}{\lambda}(X-ct)\right]; \quad \text{upper wall},$$
$$Y = h_2'(X,Y,t) = -d_2 - b_1\cos\left[\frac{2\pi}{\lambda}(X-ct)+\phi\right]; \quad \text{lower wall}. \tag{1}$$

In the above equations a_1, b_1 are the wave amplitudes, λ is the wavelength and ϕ $(0 \leqslant \phi \leqslant \pi)$ is the phase difference. When $\phi = 0$ it corresponds to symmetric channel with waves out of phase and when $\phi = \pi$ it corresponds to the situation when waves are in phase and

$$a_1^2 + b_1^2 + 2a_1b_1\cos\phi \leqslant (d_1+d_2)^2.$$

We have an interest in carrying out the flow analysis in wave frame (x',y'). The coordinates and the velocities in the laboratory (X',Y') and wave (x',y') frames are related by the following equations

$$x' = X' - ct', \quad y' = Y',$$
$$u'(x',y') = U' - c, \quad v'(x',y') = V', \tag{2}$$

in which (U',V') and (u',v') are the respective velocities in the laboratory and wave frames. A constant magnetic field of strength H_0' is applied in the transverse direction. This gives rise to an induced magnetic field $H'(h_{X'}'(X',Y',t'), h_{Y'}'(X',Y',t'),0)$ and hence the total magnetic field becomes $H'^{+}(h_{X'}'(X',Y',t'). H_0' + h_{Y'}'(X',Y',t'),0)$.

The fundamental equations governing the flow in the present problem are

$$\nabla\cdot\mathbf{H}' = 0, \quad \nabla\cdot\boldsymbol{\epsilon}' = 0, \tag{3}$$
$$\nabla\times\mathbf{H}' = \mathbf{J}', \quad \mathbf{J}' = \sigma\{\boldsymbol{\epsilon}' + \mu_e(\mathbf{V}'\times\mathbf{H}'^{+})\}, \tag{4}$$
$$\nabla\times\boldsymbol{\epsilon}' = -\mu_e\frac{\partial\mathbf{H}'}{\partial t'}, \tag{5}$$
$$\nabla\cdot\overline{\mathbf{V}'} = 0, \tag{6}$$
$$\rho\left[\frac{\partial}{\partial t'} + (\mathbf{V}'\cdot\nabla)\right]\overline{\mathbf{V}'} = -\nabla p' + \mathrm{div}\overline{\boldsymbol{\tau}'} - \mu_e\left\{(\mathbf{H}'^{+}\cdot\nabla) - \frac{1}{2}(H'^{+})^2\nabla\right\}, \tag{7}$$
$$\rho C_p\frac{dT}{dt} = \kappa\nabla^2 T + \boldsymbol{\tau}_1\cdot\mathbf{L}. \tag{8}$$

In the above expressions $\boldsymbol{\tau}_1$ is the Cauchy stress tensor, $\mathbf{L} = grad\mathbf{V}$, p' the pressure, $\mathbf{J}$ the current density, μ_e magnetic permeability, σ the electrical conductivity, $\boldsymbol{\epsilon}'$ electric field, C_p the specific heat at a constant volume, $\kappa$the thermal conductivity and T the temperature. The velocity $\mathbf{V}'$ is defined by

$$\overline{\mathbf{V}'} = (u', v', 0) \tag{9}$$

and an extra stress tensor $\bar{\boldsymbol{\tau}}$ is

$$\bar{\boldsymbol{\tau}} = -\left[\eta_0(1 + (\Gamma\bar{\dot{\gamma}})^2)^{\frac{n-1}{2}}\right]\bar{\dot{\gamma}}, \tag{10}$$
$$\bar{\dot{\gamma}} = \sqrt{\frac{1}{2}\sum_i\sum_j\bar{\dot{\gamma}}_{ij}\bar{\dot{\gamma}}_{ji}} = \sqrt{\frac{1}{2}\pi},$$

where η_0 is zero shear-rate viscosity, Γ the time constant, n the dimensionless power law index, π the second invariant of strain-rate tensor and infinite shear stress viscosity is absent. When $n = 1$ or $\Gamma = 0$; Eq. (3) reduces to a viscous fluid.

Induction equation after using Eqs. (3)–(5) takes the form

$$\frac{\partial\mathbf{H}'^{+}}{\partial t'} = \nabla\times\{\mathbf{V}'\times\mathbf{H}'^{+}\} + \frac{1}{\zeta}\nabla^2\mathbf{H}'^{+} \tag{11}$$

in which $\zeta = 1/\sigma\mu_e$ is the magnetic diffusivity.

Defining

$$x = \frac{2\pi x'}{\lambda}, \quad y = \frac{y'}{d_1}, \quad u = \frac{u'}{c}, \quad v = \frac{v'}{c}, \quad t = \frac{2\pi t'c}{\lambda}, \quad p = \frac{2\pi d_1^2 p'}{c\lambda\mu}, \quad \mathrm{Re} = \frac{\rho ca}{\mu},$$
$$\tau = \frac{d_1\tau'}{\mu c}, \quad h_1 = \frac{h_1'}{d_1}, \quad h_1 = \frac{h_1'}{d_1}, \quad \Psi = \frac{\Psi'}{cd_1}, \quad \Phi = \frac{\Phi'}{H_0d_1} \quad \delta = \frac{2\pi d_1}{\lambda}, \quad S_t = \frac{H_0}{c}\sqrt{\frac{\mu_e}{\rho}},$$
$$R_m = \sigma\mu_e ac, \quad d = \frac{d_2}{d_1}, \quad a = \frac{a_1}{d_1}, \quad b = \frac{a_2}{d_1}, \quad \theta = \frac{T-T_0}{T_1-T_0}, \quad \mathrm{Pr} = \frac{\rho\nu C_p}{\kappa}, \quad E = \frac{c^2}{C_p(T_1-T_0)}, \tag{12}$$

Eqs. (7) and (11) give

$$\mathrm{Re}\delta\left\{\left(\frac{\partial\Psi}{\partial y}\frac{\partial}{\partial x}-\frac{\partial\Psi}{\partial x}\frac{\partial}{\partial y}\right)\frac{\partial\Psi}{\partial y}\right\}=-\frac{\partial p_m}{\partial x}+\delta\frac{\partial\tau_{xx}}{\partial x}+\frac{\partial\tau_{xy}}{\partial y}+\mathrm{Re}\delta S_t^2\left(\frac{\partial\Phi}{\partial y}\frac{\partial}{\partial x}-\frac{\partial\Phi}{\partial x}\frac{\partial}{\partial y}\right)\frac{\partial\Phi}{\partial y}+\mathrm{Re}S_t^2\frac{\partial^2\Phi}{\partial y^2}, \tag{13}$$

$$-\mathrm{Re}\delta^3\left\{\left(\frac{\partial\Psi}{\partial y}\frac{\partial}{\partial x}-\frac{\partial\Psi}{\partial x}\frac{\partial}{\partial y}\right)\frac{\partial\Psi}{\partial x}\right\}=-\frac{\partial p_m}{\partial y}+\delta^2\frac{\partial\tau_{xy}}{\partial x}+\delta\frac{\partial\tau_{yy}}{\partial x}-\mathrm{Re}\delta^3S_t^2\left(\frac{\partial\Phi}{\partial y}\frac{\partial}{\partial x}-\frac{\partial\Phi}{\partial x}\frac{\partial}{\partial y}\right)\frac{\partial\Phi}{\partial x}-\mathrm{Re}\delta^2S_t^2\frac{\partial^2\Phi}{\partial x\partial y}, \tag{14}$$

$$\frac{\partial\Psi}{\partial y}-\delta\left(\frac{\partial\Psi}{\partial y}\frac{\partial\Phi}{\partial x}-\frac{\partial\Psi}{\partial x}\frac{\partial\Phi}{\partial y}\right)+\frac{1}{R_m}\nabla^2\Phi=E, \tag{15}$$

$$\frac{\partial^2\theta}{\partial y^2}+Br\left\{1+\frac{(n-1)}{2}We^2\dot{\gamma}^2\right\}\left(\frac{\partial^2\Psi}{\partial y^2}-\delta^2\frac{\partial^2\Psi}{\partial x^2}\right)\frac{\partial^2\Psi}{\partial y^2}=0, \tag{16}$$

where

$$u=\frac{\partial\Psi}{\partial y},\quad v=-\delta\frac{\partial\Psi}{\partial x},\quad h_x=\frac{\partial\Phi}{\partial y},\quad h_y=-\delta\frac{\partial\Phi}{\partial x},$$

$$p_m=p+\frac{1}{2}\mathrm{Re}\delta\frac{\mu_e(H'^{+})^2}{\rho c^2},\quad Br=E\mathrm{Pr}. \tag{17}$$

$$\nabla^2=\delta^2\frac{\partial^2}{\partial x^2}+\frac{\partial^2}{\partial y^2}, \tag{18}$$

$$\tau_{xx}=-2\left[1+\frac{(n-1)}{2}We^2\dot{\gamma}^2\right]\frac{\partial^2\Psi}{\partial x\partial y}, \tag{19}$$

$$\tau_{xy}=-\left[1+\frac{(n-1)}{2}We^2\dot{\gamma}^2\right]\left(\frac{\partial^2\Psi}{\partial y^2}-\delta^2\frac{\partial^2\Psi}{\partial x^2}\right), \tag{20}$$

$$\tau_{yy}=2\delta\left[1+\frac{(n-1)}{2}We^2\dot{\gamma}^2\right]\frac{\partial^2\Psi}{\partial x\partial y}, \tag{21}$$

$$\dot{\gamma}=\left[2\delta^2\left(\frac{\partial^2\Psi}{\partial x\partial y}\right)^2+\left(\frac{\partial^2\Psi}{\partial y^2}-\delta^2\frac{\partial^2\Psi}{\partial x^2}\right)^2+2\delta^2\left(\frac{\partial^2\Psi}{\partial x\partial y}\right)^2\right]^{\frac{1}{2}}. \tag{22}$$

Here δ is a wave number, We the Weissenberg number, S_t the Strommer's number, Re the Reynolds number, R_m the magnetic Reynolds number, p_m the magnetic pressure, M the Hartman number, Pr the Prandtl number, E the Eckert number and Br the Brickman number.

Eqs. (13)–(16) after invoking long wavelength approximation yield [2,7,10–15]:

$$\frac{\partial p}{\partial x}=\frac{\partial}{\partial y}\left[\left\{1+\frac{(n-1)}{2}We^2\left(\frac{\partial^2\Psi}{\partial y^2}\right)^2\right\}\frac{\partial^2\Psi}{\partial y^2}\right]+M^2\left(\epsilon-\frac{\partial\Psi}{\partial y}\right), \tag{23}$$

$$\frac{\partial p}{\partial y}=0, \tag{24}$$

$$\frac{\partial\Psi}{\partial y}+\frac{1}{R_m}\frac{\partial^2\Phi}{\partial y^2}=E, \tag{25}$$

$$\frac{\partial^2\theta}{\partial y^2}+Br\left[\left\{1+\frac{(n-1)}{2}We^2\left(\frac{\partial^2\Psi}{\partial y^2}\right)^2\right\}\left(\frac{\partial^2\Psi}{\partial y^2}\right)^2\right]=0, \tag{26}$$

where Eq. (24) shows that $p\neq p(y)$ and hence $p=p(x)$.

With the help of Eqs. (23) and (24) we obtain

$$\frac{\partial^2}{\partial y^2}\left[\left\{1+\frac{(n-1)}{2}We^2\left(\frac{\partial^2\Psi}{\partial y^2}\right)^2\right\}\frac{\partial^2\Psi}{\partial y^2}\right]-M^2\frac{\partial^2\Psi}{\partial y^2}=0. \tag{27}$$

The dimensionless boundary conditions [5,6,15] and pressure rise per wavelength (Δp_λ) are

$$\Psi = \frac{F}{2}, \quad \frac{\partial \Psi}{\partial y} = -1, \quad \Phi = 0, \quad \theta' = 0 \quad \text{at } y = h_1 = 1 + a\cos 2\pi x,$$
$$\Psi = -\frac{F}{2}, \quad \frac{\partial \Psi}{\partial y} = -1, \quad \Phi = 0, \quad \theta' = 1 \quad \text{at } y = h_2 = -d - b\cos(2\pi x + \phi), \tag{28}$$
$$\Delta p_\lambda = \int_0^{2\pi} \left(\frac{dp}{dx}\right)\Big|_{y=0} dx. \tag{29}$$

The dimensionless mean flows in laboratory (θ) and wave (F) frames are related by the following expressions

$$\theta = F + d + 1, \tag{30}$$
$$F = \int_{h_2(x)}^{h_1(x)} \frac{\partial \Psi}{\partial y} dy = \Psi(h_1(x)) - \Psi(h_2(x)). \tag{31}$$

3. Perturbation solution

For series solution we write

$$\Psi = \Psi_0 + We^2 \Psi_1 + O(We^4), \tag{32}$$
$$\Phi = \Phi_0 + We^2 \Phi_1 + O(We^4), \tag{33}$$
$$F = F_0 + We^2 F_1 + O(We^4), \tag{34}$$
$$p = p_0 + We^2 p_1 + O(We^4). \tag{35}$$

Upon making use of above equations into Eqs. (23) and (25), (26), (27), (28) and then solving the resulting systems and retaining the terms of $O(We^2)$, we have

$$\begin{aligned}
\Psi = {} & \frac{1}{128L_1^3}\Big(M^4(-1+n)We^2(h_1-h_2)^3(2(-\cosh(M(3y-h_1-2h_2)) + \cosh(M(y+h_1-2h_2)) + \cosh(M(3y-2h_1-h_2)) \\
& - \cosh(M(y-2h_1+h_2)) + 2My(-6\sinh(M(y-h_1)) + 6\sinh(M(y-h_2)) - 8\sinh(M(h_1-h_2)) \\
& + \sinh(2M(h_1-h_2)))\Big) + M(12M(-1+\cosh(M(y+h_2)))h_1^2 - (24My - 12My(\cosh(M(y+h_1)) \\
& + \cosh(M(y+h_2))) - 12\sinh(M(y-h_1)) + \sinh(M(3y-h_1-2h_2)) - 3\sinh(M(y+h_1-2h_2)) \\
& + 12\sinh(M(y-h_2)) + \sinh(M(3y-2h_1-h_2)) - 16\sinh(M(h_1-h_2)) + 2\sinh(2M(h_1-h_2)) \\
& - 3\sinh(M(y-2h_1+h_2)) + 12M(-1+\cosh(M(y+h_1))h_2) + h_1(24My - 12My(\cosh(M(y+h_1)) \\
& + \cosh(M(y+h_2))) + 12\sinh(M(y-h_1)) + \sinh(M(3y-h_1-2h_2)) - 3\sinh(M(y+h_1-2h_2)) \\
& - 12\sinh(M(y-h_2)) + \sinh(M(3y-2h_1-h_2)) + 12\sinh(M(h_1-h_2)) - 2\sinh(2M(h_1-h_2)) \\
& - 3\sinh(M(y-2h_1-h_2)) + 12M(\cosh(M(y-h_1)) - \cosh(M(y+h_2))h_2)))) + \frac{1}{L_3L_4}\Big(2\cosh(M(y+h_1))(\cosh(My) \\
& - \sinh(My))\sinh\left(\frac{M}{2}(y-h_2)\right)\left(\cosh\left(\frac{M}{2}(2y+h_1+h_2)\right) + \sinh\left(\frac{M}{2}(2y+h_1+h_2)\right)\right) \\
& + \frac{h_1F}{4}(\cosh(My) - \sinh(My))(2(\cosh(2My) - My\cosh(M(y+h_1)) - My\cosh(M(y+h_2)) - \cosh(M(h_1+h_2)) \\
& + \sinh(2My) - My\sinh(M(y+h_1)) - My\sinh(M(y+h_2)) - \sinh(M(h_1+h_2)) + M(\cosh(M(y+h_1)) \\
& + \sinh(M(y+h_1)) + \sinh(M(y+h_2)))h_1 + \sinh(M(y+h_2))h_2) + (-\cosh(My) \\
& + \sinh(My)(y(\cosh(M(y+h_1)) - \cosh(M(y+h_2)) + \sinh(M(y+h_1)) - \sinh(M(y+h_2)) \\
& + 2\cosh\left(\frac{M}{2}(y-h_2)\right)\sinh\left(\frac{M}{2}(y-h_1)\right)\left(\cosh\left(\frac{M}{2}(2y+h_1+h_2)\right) + \sinh\left(\frac{M}{2}(2y+h_1+h_2)\right)\right)h_2\Big)\Big)\Big)\Big)\Big)\Big)\Big), \qquad (36)
\end{aligned}$$

$$\begin{aligned}
\frac{dp}{dx} = {} & \left(\frac{M^2}{L_5}(-2(1+\epsilon)\sinh\left(\frac{M}{2}(h_1+h_2)\right) - \cosh\left(\frac{M}{2}(h_1+h_2)\right)(F - \epsilon h_1 + \epsilon h_2))\right) \\
& + \frac{1}{128L_1^3}\Big(We^2(192M^7(-1+n)\cosh\left(\frac{M}{2}(h_1+h_2)\right)\left(\sinh\left(\frac{M}{2}(h_1+h_2)\right)\right)^2(F+h_1-h_2)^3 \\
& + \frac{1}{L_1}\Big(M^7(-1+n)(h_1-h_2)^3(-24\sinh(Mh_1) + 32\sinh(M(h_1-h_2)) - 4\sinh(2M(h_1-h_2)) \\
& + 24\sinh(Mh_2) - 2\sinh(M(h_1-2h_2)) - 2\sinh(M(2h_1-h_2)) + 6\sinh(M(2h_1+h_2)) \\
& - 6\sinh(M(h_1+2h_2)) - 3M(-4M\sinh(Mh_2)h_1^2 + h_2(-8 + 8\cosh(Mh_1) + \cosh(M(h_1-2h_2))
\end{aligned}$$

$$+\cosh(M(2h_1-h_2))-\cosh(M(2h_1+h_2))-\cosh(M(h_1+2h_2))+4M\sinh(Mh_1)h_2)$$
$$+h_1(8-8\cosh(Mh_2)-\cosh(M(h_1-2h_2))-\cosh(M(2h_1-h_2))+\cosh(M(2h_1+h_2))$$
$$+\cosh(M(h_1+2h_2))-4M\sinh(Mh_1)h_2+4M\sinh(Mh_2)h_2)))\Big)+\frac{1}{L_1}\Big(M^7(-1+n)(h_1-h_2)^3(-72\sinh(Mh_1)$$
$$-72\sinh(Mh_2)+2\sinh(M(h_1-2h_2))+2\sinh(M(2h_1-h_2))-54\sinh(M(2h_1+h_2))$$
$$+54\sinh(M(h_1+2h_2))+3M(-4M\sinh(Mh_2)h_1^2+h_2(16\cosh(Mh_1)+8\cosh(Mh_2)+\cosh(M(h_1-2h_2))$$
$$+\cosh(M(2h_1-h_2))-9\cosh(M(2h_1+h_2))-9\cosh(M(h_1+2h_2))+4M\sinh(Mh_1)h_2)$$
$$+h_1(-8\cosh(Mh_1)-16\cosh(Mh_2)-\cosh(M(h_1-2h_2))-\cosh(M(2h_1-h_2))+9\cosh(M(2h_1+h_2))$$
$$+9\cosh(M(h_1+2h_2))-4\sinh(Mh_1)h_2+4M\sinh(Mh_2)h_2)))))). \tag{37}$$

The expressions of magnetic force function $\Phi$and axial induced magnetic field h_x are

$$\Phi=\frac{1}{384L_1^4M^2}\Big(\Big(\Big(64L_1^3M\Big(F(6+My(12+My(3+2My))\Big)\Big)\cosh\Big(\frac{M}{2}(h_1-h_2)\Big)-6F\Big(\cosh\Big(\frac{M}{2}(2y-h_1-h_2)\Big)$$
$$+2\sinh\Big(\frac{M}{2}(2y-h_1-h_2)\Big)\Big)+6(My^2+F(-2+My))\sinh\Big(\frac{M}{2}(h_1-h_2)\Big)$$
$$+64L_1^3M\Big(6\cosh\Big(\frac{M}{2}(2y-h_1-h_2)\Big)h_2-6M(F+y)\sinh\Big(\frac{M}{2}(h_1-h_2)\Big)h_2$$
$$+\cosh\Big(\frac{M}{2}(h_1-h_2)\Big)h_2(-3(2+FM(4+M^2y^2))+FM^2h_2(-3+Mh_2))+3M\epsilon(y^2-h_2^2)L_1\Big)$$
$$+\Big(2(36My\cosh(M(y-h_1))-36My\cosh(M(y-h_2))-36\sinh(M(y-h_1))+\sinh(M(3y-h_1-2h_2))$$
$$-\sinh(M(y+h_1-2h_2))+36\sinh(M(y-h_2))-\sinh(M(3y-2h_1-h_2))+36\sinh(M(y-h_2))$$
$$-\sinh(M(3y-2h_1-h_2))+8(-4+3M^2y^2)\sinh(M(h_1-h_2))+(2-3M^2y^2)\sinh(2M(h_1-h_2))$$
$$+3\sinh(M(y-2h_1+h_2))\Big)+Mh_2\Big(\cosh(M(3y-h_1-2h_2))-9\cosh(M(y+h_1-2h_2))+72\cosh(M(y-h_2))$$
$$-64\cosh(M(h_1-h_2))+\cosh(2M(h_1-h_2))-9\cosh(M(y-2h_1+h_2))+6My(-6(-My+\sinh(M(y-h_1))$$
$$+\sinh(M(y-h_2))\Big)-8\sinh\Big(M(h_1-h_2))(-2-My(1+My)+Mh_2(1+Mh_2))+2M\epsilon(-y+h_2)L_1)$$
$$-(72\cosh(M(y-h_1))+\cosh(M(3y-h_1-2h_2))-9\cosh(M(y+h_1-2h_2))+\cosh(M(3y-2h_1-h_2))$$
$$-64\cosh(M(h_1-h_2))+6\cosh(2M(h_1-h_2))+6Mh_2(6\sinh(M(y-h_1))-6\sinh(M(y-h_2))$$
$$-8\sinh(M(h_1-h_2))-6Mh_2))L_2)+12M^2h_1^2(-3\sinh(M(y-h_2))L_2$$
$$+M(y-h_2)\Big(64L_1^3\sinh\Big(\frac{M}{2}(h_1-h_2)\Big)+3L_2\Big)\Big)\Big)R_m\Big)\Big)\Big), \tag{38}$$

$$h_x=\frac{1}{128L_1^4M}\Big(\Big(\Big(128L_1^3M(F(2+My(1+My))\cosh\Big(\frac{M}{2}(h_1-h_2)\Big)-F\Big(2\cosh\Big(\frac{M}{2}(2y-h_1-h_2)\Big)$$
$$+\sinh\Big(\frac{M}{2}(2y-h_1-h_2)\Big)+(F+2y)\sinh\Big(\frac{M}{2}(h_1-h_2)\Big)+128L_1^3M\Big(-2\cosh\Big(\frac{M}{2}(2y-h_1-h_2)\Big)h_1$$
$$-\sinh\Big(\frac{M}{2}(2y-h_1-h_2)\Big)h_1+\sinh\Big(\frac{M}{2}(2y-h_1-h_2)\Big)h_2-\sinh\Big(\frac{M}{2}(h_1-h_2)\Big)(h_1(1+2My-2Mh_1)+h_2)$$
$$-\cosh\Big(\frac{M}{2}(h_1-h_2)\Big)((-2+FM(1+My))h_1+FM^2(y-h_1)h_2)+y\epsilon L_1-h_1\epsilon L_1\Big)$$
$$+2\Big(\cosh(M(3y-h_1-2h_2))-\cosh(M(y+h_1-2h_2))-\cosh(M(3y-2h_1-h_2))+\cosh(M(y-2h_1+h_2))L_2$$
$$+M\Big(-4y(-6\sinh(M(y-h_1))+\sinh(M(y-h_2))-8\sinh(M(h_1-h_2))+\sinh(2M(h_1-h_2))\Big)$$
$$-h_1\Big(24My-12My(\cosh(M(y-h_1))+\cosh(M(y-h_2))\Big)+12\sinh(M(y-h_1))+\sinh(M(3y-h_1-2h_2))$$
$$-3\sinh(M(y+h_1-2h_2))-3\sinh(M(y+h_1-2h_2))+12\sinh(M(y-h_2))+\sinh(M(3y-2h_1-h_2))$$
$$-16\sinh(M(h_1-h_2))+2\sinh(2M(h_1-h_2))-3\sinh(M(y-2h_1-h_2))+12M(-\cosh(M(y-h_2))h_1)h_2$$
$$+12M(-1+\cosh(M(y-h_1)))h_2^2)L_2\Big)R_m\Big)\Big)\Big)\Big)\Big). \tag{39}$$

Expression of temperature is

$$\theta' = \left(L_8 - \left(\frac{1}{262144 L_1 M^2 L_6^4}\left(\left(\left(BrWe^2\left(16384F^4L_1^6L_2^2M^8L_9 - 65536F^3F_1^6L_2^2M^8L_{10} + 9830F^2L_1^6L_2^2M^8L_{11}\right.\right.\right.\right.\right.$$
$$- 65536FL_1^6L_2^2M^8L_{12} + 16384L_1^6L_2^2M^8L_{13} - 393216L_1^6L_2^2M^{10}L_{14} + (4L_{15} + Mh_2(4L_{16} - L_{17}) + L_{18} + 4(L_{19} + L_{20}))\Big)L_6^4L_7^2\Big)$$
$$- 32M^4h_1^4(512L_1^6L_2^2M^4L_{21} + 3L_{22}L_6^4L_7^2) + 4M^3h_1^3\Big(16384L_1^6L_2^2M^5L_{23}L_{24} + L_{25} + L_{26} - L_{27}\Big)L_6^4L_7^2$$
$$- 3M^2h_1^2\Big(32768L_1^6L_2^2M^6L_{28}L_{29}\Big) + L_{30} + 4Mh_2L_{31}\Big)L_6^4L_7^2 - 2Mh_1\Big(327268F^3L_1^6L_2^2L_{32}$$
$$\left.\left.\left.\left.\left. + 98304F^2L_1^6L_2^2L_{32}L_{33} + 98304FL_1^6L_2^2L_{32}L_{34} + 32768L_1^6L_2^2L_{32}L_{35} + 19660L_1^6L_2^2L_{36} - L_{37} + L_{38} - L_{39} + L_{40} + 6Mh_2L_{41}\Big)\right)\right)\right),$$

where

$$L_1 = 2\sinh\left(\frac{M}{2}(h_1 - h_2)\right) + M\cosh\left(\frac{M}{2}(h_1 - h_2)\right)(-h_1 + h_2),$$
$$L_2 = M^5(-1 + n)(h_1 - h_2)^3,$$
$$L_3 = \cosh\left(\frac{M}{2}(h_1 + h_2)\right) + \sinh\left(\frac{M}{2}(h_1 + h_2)\right),$$
$$L_4 = 2\sinh\left(\frac{M}{2}(h_1 - h_2)\right) - M\cosh\left(\frac{M}{2}(h_1 + h_2)\right)h_1 + M\cosh\left(\frac{M}{2}(h_1 - h_2)\right)h_2,$$
$$L_5 = -2\sinh\left(\frac{M}{2}(h_1 - h_2)\right) + M\cosh\left(\frac{M}{2}(h_1 - h_2)\right)(h_1 - h_2),$$
$$L_6 = 4\sinh\left(\frac{M}{2}(h_1 - h_2)\right) + 2M\cosh\left(\frac{M}{2}(h_1 - h_2)\right)(-h_1 + h_2),$$
$$L_7 = M^6(-1 + n)(h_1 - h_2)^3,$$

$$L_8 = \frac{1}{2(h_1 - h_2)L_6^2}(2BrM^4h_1^4(-y + h_2) + BrM^2h_2(-F + h_2)^2(-2M^2y^2 - \cosh(M(h_1 - h_2)) + \cosh(2My - M(h_1 - h_2))$$
$$+ 2M^2yh_2 + BrM^2h_1(-F + h_2)((-2M^2y^2 - \cosh(M(h_1 - h_2)) + \cosh(2My - M(h_1 - h_2))F$$
$$+ 3(2M^2y^2 + \cosh(M(h_1 - h_2)) - \cosh(2My - M(h_1 - h_2))h_2 + 2M^2(F - 2y)h_2^2 - 2M^2h_2^3$$
$$+ BrM^2h_1^2\Big(-2F(M^2(F - 2y)y - \cosh(M(h_1 - h_2)) + \cosh(2My - M(h_1 - h_2)))$$
$$+ (2M^2(F - y)(F + 3y) - 3\cosh(M(h_1 - h_2)) + \cosh(2My - M(h_1 + h_2)) - 8M^2Fh_2^2 + 6M^2h_2^3)$$
$$+ BrM^2h_1^3(2M^2y(-F + y) - \cosh(2My - M(h_1 - h_2)) + 2M^2(2(F + y) - 3h_2)) + 2(-y + h_1)L_6^2\Big)\Big)\Big)\Big)\Big)\Big),$$

$$L_9 = (-1 + n)(24M^2y^2 + 16\cosh(M(h_1 - h_2)) - \cosh(2M(h_1 - h_2)) + \cosh(4My - 2M(h_1 - h_2)) - 16\cosh(2My$$
$$- M(h_1 + h_2))),$$

$$L_{10} = (-1 + n)(6M^2y(F + 4y) + 16\cosh(M(h_1 - h_2)) - \cosh(2M(h_1 - h_2)) + \cosh(4My - 2M(h_1 + h_2))$$
$$- 16\cosh(2My - M(h_1 + h_2))h_2),$$

$$L_{11} = (-1 + n)(8M^2y(2F + 3y) + 16\cosh(M(h_1 - h_2)) - 16\cosh(2M(h_1 - h_2)) + \cosh(4My - 2M(h_1 + h_2))$$
$$- 16\cosh(2My - M(h_1 + h_2))h_2^2),$$

$$L_{12} = (-1 + n)(12M^2y(3F + 2y) + 16\cosh(M(h_1 - h_2)) - \cosh(2M(h_1 - h_2)) + \cosh(4My - 2M(h_1 + h_2))$$
$$- 16\cosh(2My - M(h_1 + h_2))h_2^3),$$

$$L_{13} = (-1 + n)(24M^2y(4F + y) + 16\cosh(M(h_1 - h_2)) - M^2y^2) + \cosh(4My - 2M - 2M(h_1 + h_2))$$
$$- 16\cosh(2My - M(h_1 + h_2))h_2^4,$$

$$L_{14} = (-1 + n)yh_2^5,$$

$$
\begin{aligned}
L_{15} = {} & (-1635 + 5264M^2y^2 - 192M^4y^4 + 12(137 + 24M^2y^2)\cosh(2M(y-h_2)) - 9\cosh(4M(y-h_1)) \\
& - 153\cosh(M(4y-h_1-3h_2)) + 84\cosh(M(2y+h_1-3h_2)) + 18\cosh(2M(3y-h_1-2h_2)) \\
& + 2\cosh(2M(y+h_1-2h_2)) + 12(137 + 24M^2y^2)\cosh(2M(y-h_2)) - 9\cosh(4M(y-h_2)) \\
& - 153\cosh(M(4y-3h_1-h_2)) + 18\cosh(2M(3y-2h_1-h_2)) - 3460\cosh(M(2y-h_1-h_2)) \\
& - 576M^2y^2\cosh(M(2y-h_1-h_2)) + 324\cosh(2M(2y-2h_1-h_2)) - 36\cosh(3M(2y-h_1-h_2)) \\
& + (3529 - 4872M^2y^2 + 192M^4y^4)\cosh(M(h_1-h_2)) - 4(497 + 96M^2y^2)\cosh(2M(h_1-h_2)) \\
& + (105 - 8M^2y^2)\cosh(3M(h_1-h_2)) - 11\cosh(4M(h_1-h_2)) + 84\cosh(M(2y-3h_1+h_2)) \\
& + 2\cosh(2M(y-2h_1+h_2)) + 96My\sinh(2M(y-h_1)) - 108My\sinh(M(4y-h_1-3h_2)) \\
& + 48\sinh(M(2y+h_1-3h_2)) + 96My\sinh(2M(y-h_2)) - 108\sinh(M(4y-3h_1-h_2)) \\
& - 288My\sinh(M(2y-h_1-h_2)) + 216My\sinh(2M(2y-h_1-h_2)) + 48My\sinh(M(2y-3h_1+h_2))),
\end{aligned}
$$

$$
\begin{aligned}
L_{16} = {} & (-1692\sinh(2M(y-h_1)) + 18\sinh(4M(y-h_1)) - 99\sinh(M(4y-h_1-3h_2)) + 144\sinh(M(2y+h_1-3h_2)) \\
& + 6\sinh(2M(y+h_1-2h_2)) + 1594\sinh(2M(y-h_2)) - 18\sinh(4M(y-h_2)) + 207\sinh(M(4y-3h_1-h_2)) \\
& + 144\sinh(M(2y-h_1-h_2)) - 108\sinh(2M(2y-h_1-h_2)) - 534\sinh(2M(h_1-h_2)) \\
& + 4My(-96\cosh(2M(y-h_1)) - 27\cosh(M(4y-3h_1-3h_2)) + 24\cosh(M(2y+h_1-3h_2)) \\
& - 48\cosh(2M(y-h_2)) + 27\cosh(M(4y-3h_1-h_2)) + 2(72\cosh(M(2y-h_1-h_2)) \\
& + (609 - 48M^2y^2)\cosh(M(h_1-h_2)) + 48\cosh(2M(h_1-h_2)) + \cosh(3M(h_1-h_2)) \\
& - 12\cosh(M(2y-3h_1+h_2)) + 6My(-6\sinh(2M(y-h_1)) + 6\sinh(2M(y-h_2)) \\
& - (102 - 4M^2y^2 + 32\cosh(M(h_1-h_2)) + \cosh(2M(h_1-h_2)))\sinh(M(h_1-h_2))))))),
\end{aligned}
$$

$$
\begin{aligned}
L_{17} = {} & 1476\sinh(2M(h_1-h_2)) - 45\sinh(3M(h_1-h_2)) - 2(2632My - 192M^3y^3 + \sinh(4M(h_1-h_2)) \\
& + 96\sinh(2M(y-2h_1+h_2)) + 9\sinh(6My - 2M(2h_1+h_2)) - 9\sinh(6My - 2M(h_1+2h_2))),
\end{aligned}
$$

$$
\begin{aligned}
L_{18} = {} & 9\cosh(4M(y-h_1)) - 27\cosh(M(4y-h_1-3h_2)) + 36\cosh(M(2y-h_1-3h_2)) + 6\cosh(2M(y+h_1-2h_2)) \\
& + 4(253 + 24M^2y^2)\cosh(2M(y-h_2)) - 9\cosh(4M(y-h_2)) - 171\cosh(M(4y-3h_1-h_2)) \\
& - 36\cosh(2M(2y-h_1-h_2)) + 12\cosh(3M(2y-h_1-h_2)) - 293\cosh(M(h_1-h_2)) - 988\cosh(2M(h_1-h_2)) \\
& - 21\cosh(3M(h_1-h_2)) + 6\cosh(2M(y-2h_1+h_2)) + 6\cosh(2M(y-2h_1+h_2)) + 288\cosh(2My - M(h_1+h_2)) \\
& + 6\cosh(6My - 2M(2h_1+h_2)) + 6\cosh(6My - 2M(h_1+2h_2)),
\end{aligned}
$$

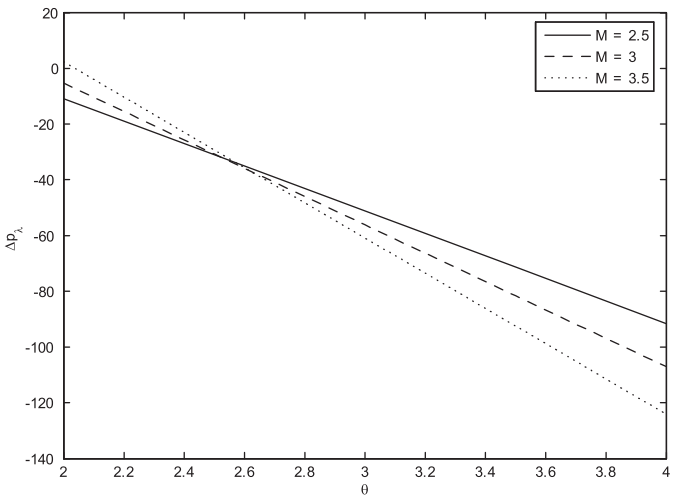

Fig. 1. Plot showing Δp_λ versus flow rate θ. Here $n = 0.398$, $We = 0.01$, $a = 0.6$, $\epsilon = 0.4$, $\phi = \frac{\pi}{6}$, $b = 0.4$ and $d = 1.1$.

$$L_{19} = ((3+48M^2y^2)\cosh(M(2y-h_1-h_2)) + My(168\sinh(2M(y-h_1)) - 9\sinh(M(4y-h_1-3h_2)) + 12\sinh(M(2y+h_1-3h_2)) + 1624\sinh(M(h_1-h_2)) + 2My((-403+8M^2y^2)\cosh(M(h_1-h_2)) - 58\cosh(2M(h_1-h_2)) - 3\cosh(3M(h_1-h_2)) - 64My\sinh(M(h_1-h_2)) + 256\sinh(2M(h_1-h_2)) + 8\sinh(3M(h_1-h_2)) - 3(8\sinh(2M(y-h_2)) + 3\sinh(M(4y-3h_1-h_2)) + 24\sinh(M(2y-h_1-h_2)) + 6\sinh(2M(2y-h_1-h_2)) - 4\sinh(M(2y-3h_1+h_2))))),$$

$$L_{20} = 4Mh_2(92My - 32M^3y^3 - 48My\cosh(2M(y-h_1)) - 48My\cosh(M(2y-h_1-h_2))112My\cosh(2M(h_1-h_2)) + 6My\cosh(3M(h_1-h_2)) - 96\sinh(2M(y-h_1)) + 24\sinh(2M(y-h_2)) + 9\sinh(M(4y-3h_1-h_2)) + 36 \times \sinh(M(2y-h_1-h_2)) + 9\sinh(2M(2y-h_1-h_2)) - 12\sinh(M(2y-3h_1+h_2)) - 24Mh_2 + 48M^3y^2h_2 + 24M \times \cosh(2M(y-h_1))h_2 - 32M^3y^2h_2^2 + 3\sinh(2M(h_1-h_2))(-11-8M^2y^2+M^2yh_2) + \sinh(M(h_1-h_2))(-57 - 72M^2y^2 + 136M^2yh_2) + 2My\cosh(M(h_1-h_2))(435 - 16M^2y^2 + 8M^2h_2^2)),$$

$$L_{21} = (-1+n)(24M^2(4F+y)y - 16\cosh(M(h_1-h_2)) + \cosh(2M(h_1-h_2)) - \cosh(4My - 2M(h_1+h_2)) + 16 \times \cosh(2My - M(h_1+h_2)) + 24M^2h_2(-4F-3y+4h_2)),$$

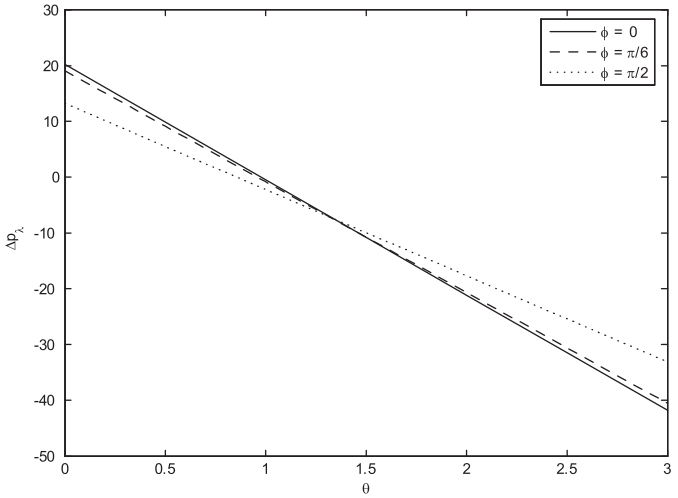

Fig. 2. Plot showing Δp_λ versus flow rate θ. Here $n = 0.398$, $We = 0.01$, $M = 1$, $\epsilon = 0.4$, $a = 0.6$, $b = 0.4$ and $d = 1.1$.

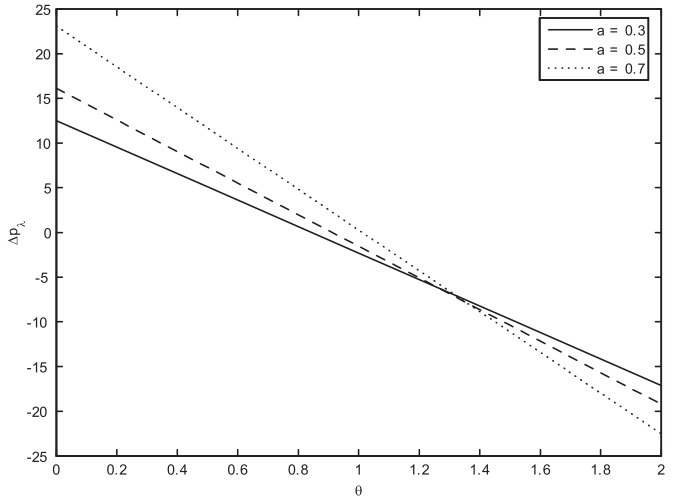

Fig. 3. Plot showing Δp_λ versus flow rate θ. Here $n = 0.398$, $We = 0.01$, $M = 1$, $\epsilon = 0.4$, $\phi = \frac{\pi}{6}$, $b = 0.4$ and $d = 1.1$.

$$L_{22} = (3 - 6M^2y^2 - 3\cosh(2M(y-h_2)) + 17M\sinh(M(h_1-h_2))(y-h_2) + 3M\sinh(2M(h_1-h_2))(y-h_2) - 8M^2yh_2 + 18M^2yh_2 + 10M^2\cosh(M(h_1-h_2))h_2(y-h_2) + 14M^2h_2^2),$$

$$L_{23} = (-1+n)(F-h_2),$$

$$L_{24} = (12M^2y(-3F+2y) + 16\cosh(M(h_1-h_2)) - \cosh(2M(h_1-h_2)) + \cosh(4My - 2M(h_1+h_2)) - 16\cosh(2My - M(h_1+h_2)) + 12M^2(3F+y-3h^2)h_2),$$

$$L_{25} = 3(92My - 32M^3y^3 - 48My\cosh(2M(y-h_2)) - 48My\cosh(M(2y-h_1-h_2)) + 24\sinh(2M(y-h_1)) + 9 \times \sinh(M(4y-h_1-3h_2)) - 12\sinh(M(2y+h_1-3h_2)) - 96\sinh(2M(y-h_2)) + 36\sinh(M(2y-h_1-h_2)) + 9 \times \sinh(2M(2y-h_1-h_2)) + 112M\cosh(2M(h_1-h_2))(y-h_2) + 6M\cosh(3M(h_1-h_2))(y-h_2) + 4Mh_2 - 96M^3y^2h_2 - 48M\cosh(2M(y-h_2)) + 48M\cosh(M(2y-h_1-h_2))h_2 - 32M^3y^2h_2^2 + 160M^3h_2^3 + \sinh(M(h_1 - h_2))(57 + 72M^2y^2 + 8M^2(50y - 59h_2)h_2)),$$

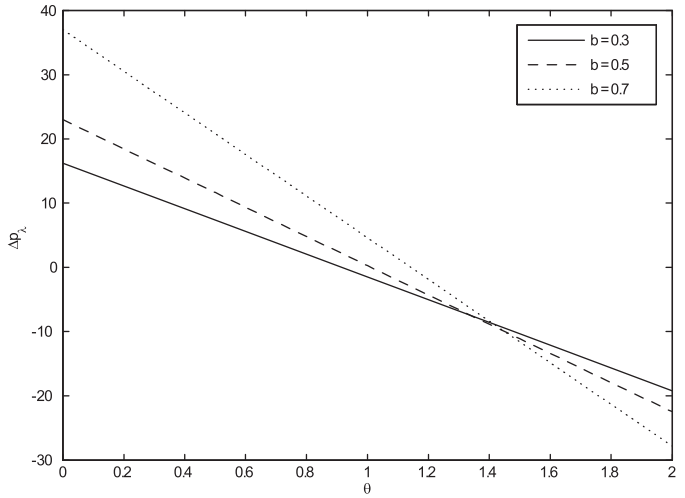

Fig. 4. Plot showing Δp_λ versus flow rate θ. Here $n = 0.398,\ We = 0.01,\ M = 1,\ \epsilon = 0.4,\ \phi = \frac{\pi}{6},\ a = 0.6$ and $d = 1.1$.

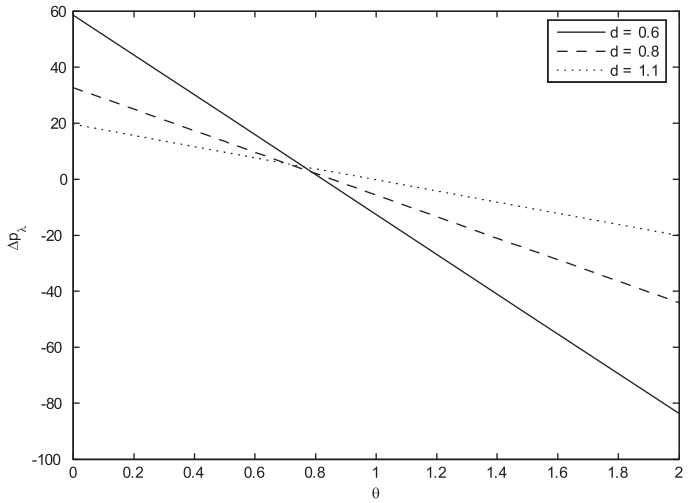

Fig. 5. Plot showing Δp_λ versus flow rate θ. Here $n = 0.398,\ We = 0.01,\ M = 1,\ \epsilon = 0.4,\ \phi = \frac{\pi}{6},\ a = 0.6$ and $b = 0.4$.

$$L_{26} = 3\sinh(2M(h_1-h_2))(11+8M^2y^2+8M^2(2y-3h_2)h_2),$$
$$L_{27} = 2M\cosh(M(h_1-h_2))(-y+h_2)(435-16M^2y^2+32M^2h_2(y+2h_2)),$$
$$L_{28} = (-1+n)(F-h_2)^2,$$

$$L_{29} = (8M^2(2F-3y)y-16\cosh(M(h_1-h_2))+\cosh(2M(h_1-h_2))-\cosh(4My-2M(h_1+h_2))+16\cosh(2My-M(h_1+h_2))+8M^2h_2(-2F+y+2h_2)),$$

$$L_{30} = 1131+624M^2y^2-64M^4y^4-4(253+24M^2y^2)\cosh(2M(y-h_1))+9\cosh(4M(y-h_1))+171\cosh(M(4y-h_1-3h_2))-164\cosh(M(2y+h_1-3h_2))-6\cosh(2M(y+h_1-2h_2))-12(95+8M^2y^2)\cosh(2M(y-h_2))+9\times\cosh(4M(y-h_2))+27\cosh(M(4y-3h_1-h_2))+36\cosh(2M(2y-h_1-h_2))-12\cosh(3M(2y-h_1-h_2))+296\cosh(M(h_1-h_2))+988\cosh(2M(h_1-h_2))+21\cosh(3M(h_1-h_2))+3\cosh(4M(h_1-h_2))-36\times\cosh(M(2y-3h_1+h_2))-288\cosh(2My-M(h_1+h_2))-6\cosh(6My-2M(2h_1+h_2))-6\cosh(6My-2M(h_1+2h_2))+4(-3(-1+18M^2y^2)\cosh(M(2y-h_1-h_2))+My(24\sinh(2M(y-h_1))+9\sinh(M(4y-h_1-3h_2))-12\sinh(M(2y+h_1-3h_2))-168\sinh(2M(y-h_2))+9\cosh(M(4y-3h_1-h_2))+72\sinh(M(2y-h_1-h_2))+18\sinh(2M(2y-h_1-h_2))+1624\sinh(M(h_1-h_2))+2My((403-8M^2y^2)\cosh(M(h_1-h_2))+56\times\cosh(2M(h_1-h_2))+3\cosh(3M(h_1-h_2))-64My\sinh(2M(h_1-h_2)))+256\sinh(2M(h_1-h_2))+8\times\sinh(3M(h_1-h_2))-12\sinh(M(2y-3h_1+h_2)))),$$

$$L_{31} = (-36My-32M^3y^3+48My\cosh(2M(y-h_1))-96My\cosh(2M(y-h_2))-48My\cosh(M(2y-h_1-h_2))+2My(499-16M^2y^2)\cosh(M(h_1-h_2))+112My\cosh(2M(h_1-h_2))+6My\cosh(3M(h_1-h_2))+48\sinh(2M(y-h_1))+18\sinh(M(4y-3h_1-h_2))+36\sinh(M(2y-h_1-h_2))+9\sinh(2M(2y-h_1-h_2))+(-1453+600M^2y^2)\sinh(M(h_1-h_2))+(157+72M^2y^2)\sinh(2M(h_1-h_2))-8\sinh(3M(h_1-h_2))+12\sinh(M(2y-3h_1+h_2))+4Mh_2(-6(-1+4M^2y^2+\cosh(2M(y-h_1))+\cosh(2M(y-h_2))-4\cosh(M(2y-h_1-h_2)))+(-451+48M^2y^2)\cosh(M(h_1-h_2))-56\cosh(2M(h_1-h_2))-3\cosh(3M(h_1-h_2))+2Mh_2(-59\sinh(M(h_1-h_2)))-9\times\sinh(2M(h_1-h_2)))-2M\cosh(M(h_1-h_2))(4y+5h_2)+2M(2y+7h_2)))),$$

$$L_{32} = (-2M^2(F^2-12y^2)+16\cosh(M(h_1-h_2))+\cosh(2M(h_1-h_2))-\cosh(4My-2M(h_1+h_2))+16\cosh(2My-M(h_1+h_2))),$$

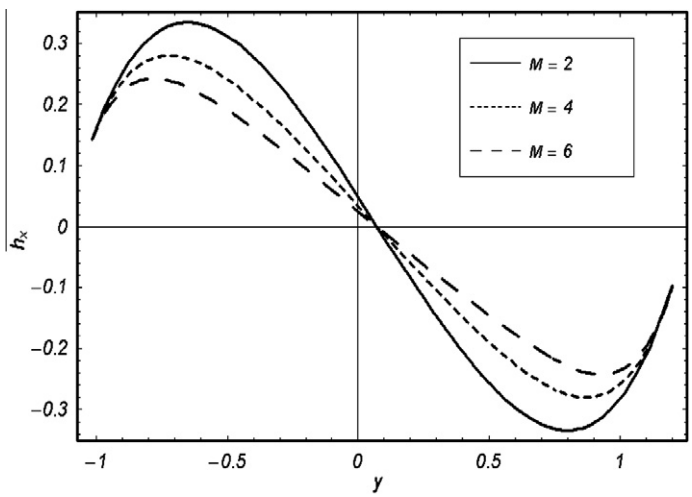

Fig. 6. Axial induced magnetic field versus y for different values of M. Here $n = 0.398$, $We = 0.01$, $a = 0.6$, $b = 0.3, d = 1.1$, $\epsilon = 0.3$, $\theta = 3$, $\phi = \frac{\pi}{6}$ and $x = 0.2$.

$$L_{33} = (-2M^2(F^2 - 12y^2) + 16\cosh(M(h_1 - h_2)) - \cosh(2M(h_1 - h_2)) + \cosh(4My - 2M(h_1 - h_2)) - 16\cosh(2My - M(h_1 + h_2)))h_2,$$

$$L_{34} = (4M^2(2F^2 - 3Fy - 6y^2) - 16\cosh(M(h_1 - h_2)) + \cosh(2M(h_1 - h_2)) - \cosh(4My - 2M(h_1 + h_2)) + 16\cosh(2My - M(h_1 + h_2)))h_2^2,$$

$$L_{35} = 12M^2(-3F^2 + 4Fy + 2y^2) + 16\cosh(2My - M(h_1 + h_2))h_2^3,$$

$$L_{36} = M^9(-1 + n)(4F - 3y)h_2^2,$$

$$L_{37} = 96608L_1^6L_2^2M^9(-1 + n)h_2^5,$$

$$L_{38} = (2(-1596\sinh(2M(y - h_1)) + 18\sinh(4M(y - h_1)) + 207\sinh(M(4y - h_1 - 3h_2)) + 192\sinh(M(2y + h_1 - 3h_2)) + 6\sinh(2M(y + h_1 - 2h_2)) + 1692\sinh(2M(y - h_2)) - 18\sinh(4M(y - h_2)) + 99\sinh(M(y - 3h_1 - h_2)) - 144 \times \sinh(M(2y - h_1 - h_2)) + 108\sinh(2M(2y - h_1 - h_2)) - 543\sinh(M(h_1 - h_2)) + 4My(48\cosh(2M(y - h_1)) - 27\cosh(M(4y - h_1 - 3h_2)) + 24\cosh(M(2y + h_1 - 3h_2)) + 96\cosh(2M(y - h_2)) + 27\cosh(M(4y - 3h_1 - h_2)) - (72\cosh(M(2y - h_1 - h_2)) + (609 - 48M^2y^2)\cosh(M(h_1 - h_2)) + 48\cosh(2M(h_1 - h_2)) + \cosh(3M(h_1 - h_2)) + 12\cosh(M(2y - 3h_1 + h_2)) + 6My(6\sinh(2M(y - h_1)) - 6\sinh(2M(y - h_2)) + (102 - 4M^2y^2 + 32\cosh(M(h_1 - h_2)) + \cosh(2M(h_1 - h_2)))\sinh(M(h_1 - h_2))))),$$

$$L_{39} = 1476\sinh(2M(h_1 - h_2)) - 45\sinh(3M(h_1 - h_2)) - 2(-2632My + 192M^3y^3 + 3\sinh(4M(h_1 - h_2)) + 72 \times \sinh(M(2y - 3h_1 + h_2)) + 3\sinh(2M(y - 2h_1 + h_2)) + 9\sinh(6My - 2M(2h_1 + h_2))),$$

$$L_{40} = Mh_2(-13921 + 48M^2y^2(9 + 4M^2y^2) + 12(221 + 24M^2y^2)\cosh(2M(y - h_1)) - 27\cosh(4M(y - h_1)) - 297 \times \cosh(M(4y + h_1 - 3h_2)) + 300\cosh(M(2y + h_1 - 3h_2)) + 18\cosh(2M(3y - h_1 - 2h_2)) + 18\cosh(2M(y + h_1 - 2h_2)) - 27\cosh(4M(y - h_2)) - 297\cosh(M(4y - 3h_1 - h_2)) + 18\cosh(2M(3y - 2h_1 - h_2)) + 2052\cosh(M(2y - h_1 - h_2)) - 108\cosh(2M(2y - h_1 - h_2)) + 36\cosh(3M(2y - h_1 - h_2)) + 8865\cosh(M(h_1 - h_2)) - 2196 \times \cosh(2M(h_1 - h_2)) - 47\cosh(3M(h_1 - h_2)) - 9\cosh(4M(h_1 - h_2)) + 300\cosh(M(2y - 3h_1 + h_2)) + 18 \times \cosh(2M(y - 2h_1 + h_2)) + 12(221 + 24M^2y^2)\cosh(2M(y - h_2)) - 56\cosh(2M(h_1 - h_2)) - 3\cosh(3M(h_1 - h_2))) + 3(24\sinh(2M(y - h_1)) - 3\sinh(M(4y - h_1 - 3h_2)) + 4\sinh(M(2y + h_1 - 3h_2)) + 24\sinh(2M(y - h_2)) - 3(\sinh(M(4y - 3h_1 - h_2)) + 8\sinh(M(2y - h_1 - h_2)) + 2\sinh(2M(2y - h_1 - h_2)) + 4\sinh(M(2y - 3h_1 + h_2)))),$$

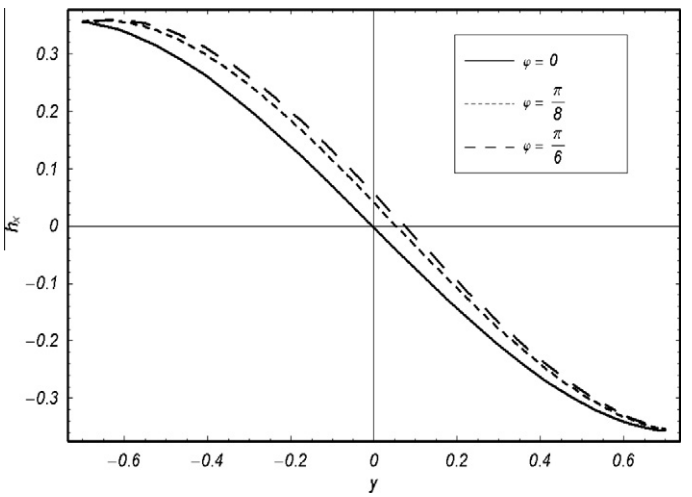

Fig. 7. Axial induced magnetic field versus y for different values of ϕ. Here $n = 0.398$, $We = 0.01$, $a = 0.6$, $b = 0.3$, $d = 1.1$, $\epsilon = 0.3$, $\theta = 3$, $M = 1$ and $x = 0.2$.

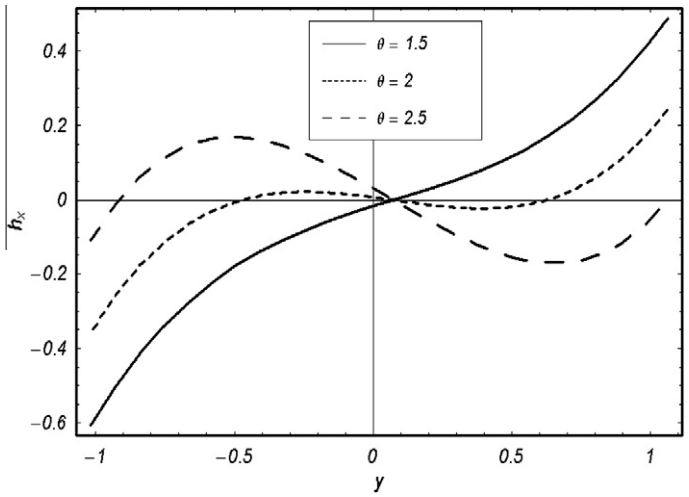

Fig. 8. Axial induced magnetic field versus y for different values of θ. Here $n = 0.398$, $We = 0.01$, $a = 0.6$, $b = 0.3$, $d = 1.1$, $\epsilon = 0.3$, $M = 1$, $\phi = \frac{\pi}{6}$ and $x = 0.2$.

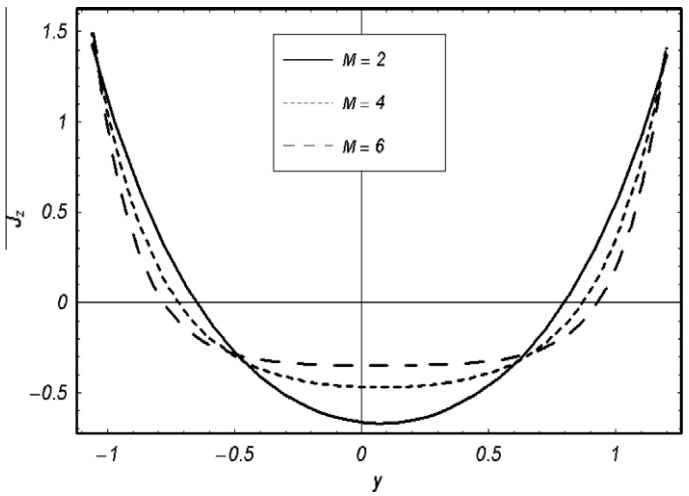

Fig. 9. Current density distribution versus y for different values of M. Here $n = 0.398$, $We = 0.01$, $a = 0.6$, $b = 0.3$, $d = 1.1$, $\epsilon = 0.3$, $\theta = 3$, $\phi = \frac{\pi}{6}$ and $x = 0.2$.

$$
\begin{aligned}
L_{41} = ((&-36My - 32M^3y^3 - 96My\cosh(2M(y-h_1)) + 48My\cosh(2M(y-h_2)) - 48My\cosh(M(2y-h_1-h_2))\\
&+ 2My(499 - 16M^2y^2)\cosh(M(h_1-h_2)) + 122M\cosh(2M(h_1-h_2)) + 6My\cosh(3M(h_1-h_2)) - 120\sinh(2M(y\\
&- h_1)) - 9\sinh(M(4y-h_1-3h_2)) + 12\sinh(M(2y+h_1-3h_2)) + 48\sinh(2M(y-h_2)) + 18\sinh(M(4y-3h_1\\
&- h_2)) + 36\sinh(M(2y-h_1-h_2)) + 9\sinh(2M(2y-h_1-h_2)) + (1453 - 600M^2y^2)\sinh(M(h_1-h_2)) + (157\\
&- 72M^2y^2)\sinh(2M(h_1-h_2)) + 8\sinh(3M(h_1-h_2)) - 24\sinh(M(2y-3h_1+h_2)) + 2Mh_2(56\cosh(2M(h_1-h_2))\\
&+ 3\cosh(3M(h_1-h_2)) - 2(1 - 24M^2y^2 - 12\cosh(2M(y-h_1)) + 12\cosh(M(2y-h_1-h_2)) + 8M^2h_2(2y+h_2))\\
&+ \cosh(M(h_1-h_2))(435 - 48M^2y^2 + 8M^2h_2(5y-h_2))))L_6^4L_7^2).
\end{aligned}
$$

4. Discussion

The main aim of this section is to study the behavior of involved key parameters on pressure rise per wave length (Δp_λ). Therefore we have prepared Figs. 1–5. The variation of Hartman number (M) on Δp_λ is displayed in Fig. 1. Here pumping rate

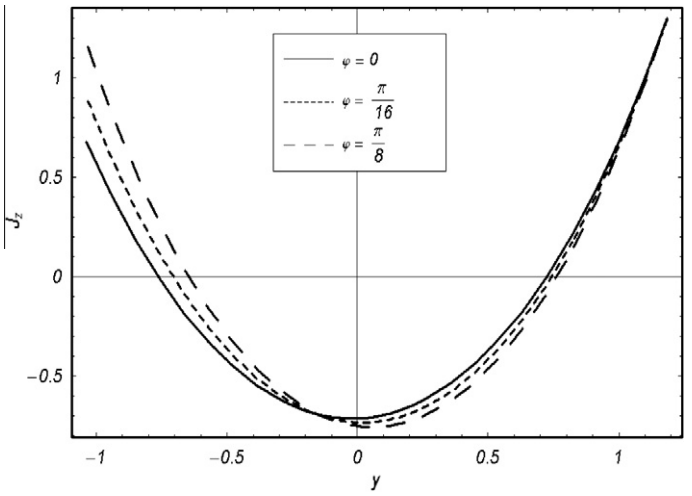

Fig. 10. Current density distribution versus y for different values of ϕ. Here $n = 0.398$, $We = 0.01$, $a = 0.6$, $b = 0.3$, $d = 1.1$, $\epsilon = 0.3$, $\theta = 3$, $M = 1$ and $x = 0.2$.

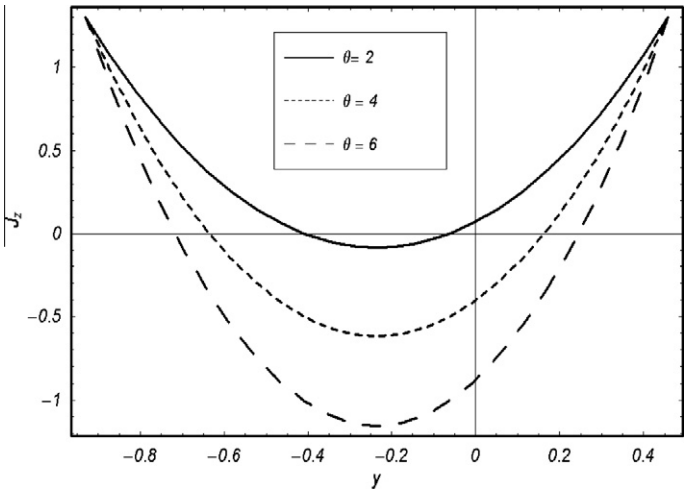

Fig. 11. Current density distribution versus y for different values of θ. Here $n = 0.398$, $We = 0.01$, $a = 0.6$, $b = 0.3$, $d = 1.1$, $\epsilon = 0.3$, $M = 1$, $\phi = \frac{\pi}{6}$ and $x = 0.2$.

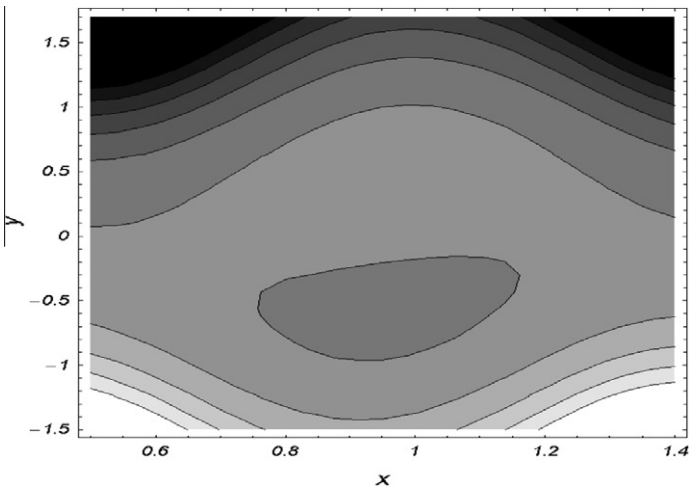

Fig. 12a. Streamlines for $M = 0.2$. The other parameters are $a = b = 0.4$, $d = 1.1$, $n = 0.498$, $We = 0.03$, $\phi = \frac{\pi}{6}$ and $\theta = 1.5$.

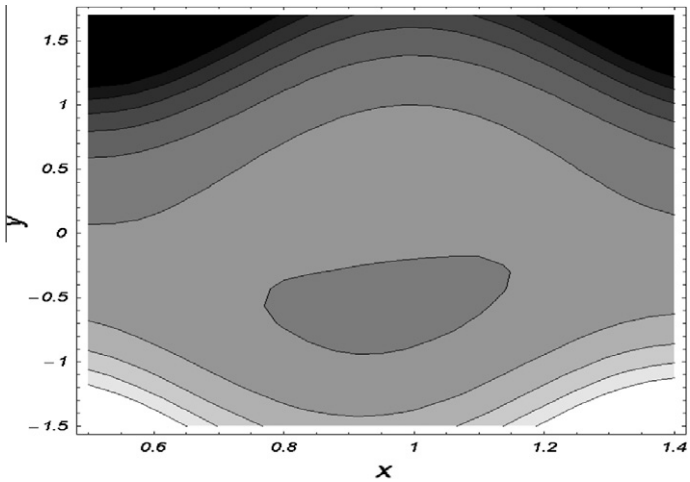

Fig. 12b. Streamlines for $M = 0.8$. The other parameters are $a = b = 0.4,\ d = 1.1,\ n = 0.498,\ We = 0.03,\ \phi = \frac{\pi}{6}$ and $\theta = 1.5$.

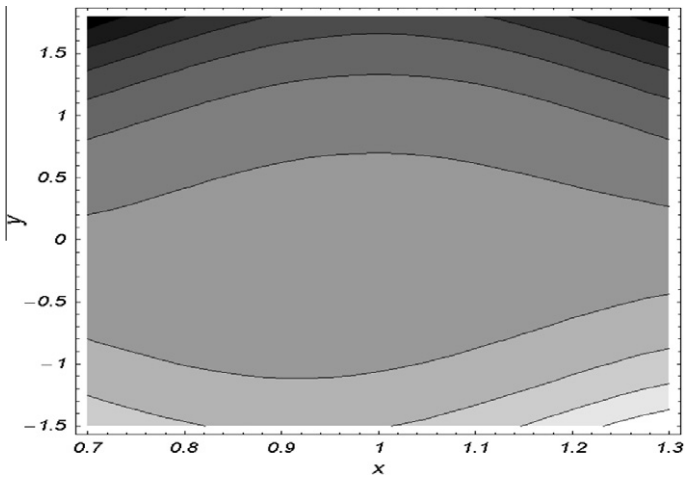

Fig. 13a. Streamlines for $\theta = 1$. The other parameters are $a = b = 0.4,\ d = 1.1,\ n = 0.498,\ We = 0.03,\ \phi = \frac{\pi}{6}$ and $M = 0.2$.

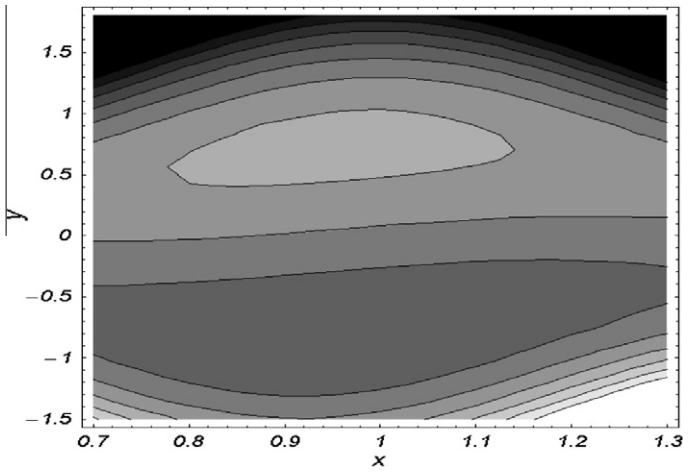

Fig. 13b. Streamlines for $\theta = 2$. The other parameters are $a = b = 0.4,\ d = 1.1,\ n = 0.498,\ We = 0.03,\ \phi = \frac{\pi}{6}$ and $M = 0.2$.

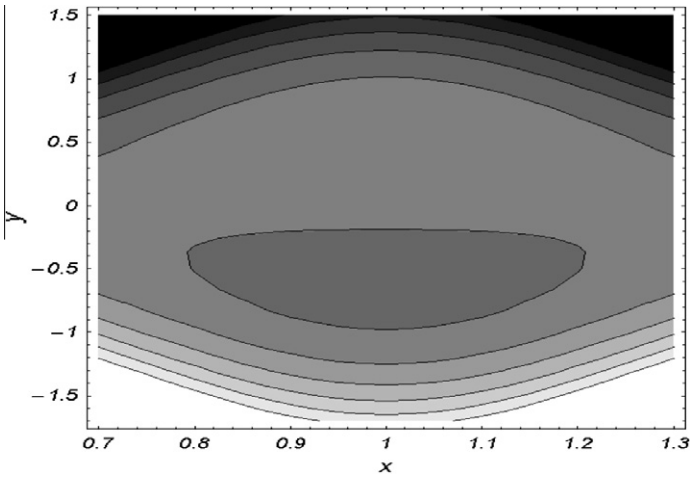

Fig. 14a. Streamlines for $\phi = 0$. The other parameters are $a = b = 0.4$, $d = 1.1$, $n = 0.498$, $We = 0.03$, $\theta = 1.5$ and $M = 0.2$.

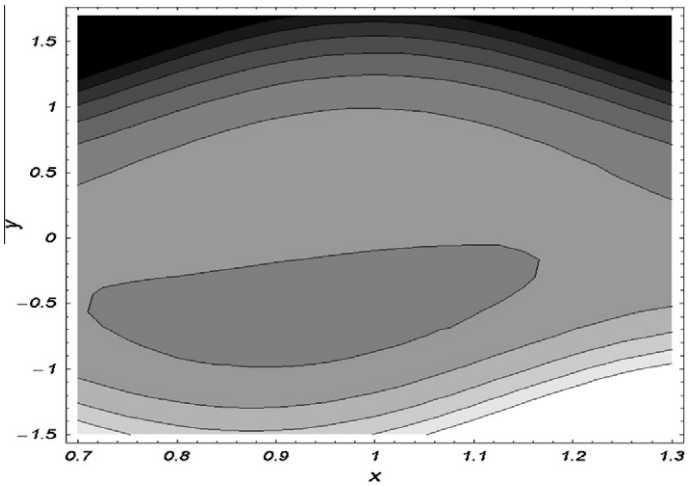

Fig. 14b. Streamlines for $\phi = \frac{\pi}{4}$. The other parameters are $a = b = 0.4$, $d = 1.1$, $n = 0.498$, $We = 0.03$, $\theta = 1.5$ and $M = 0.2$.

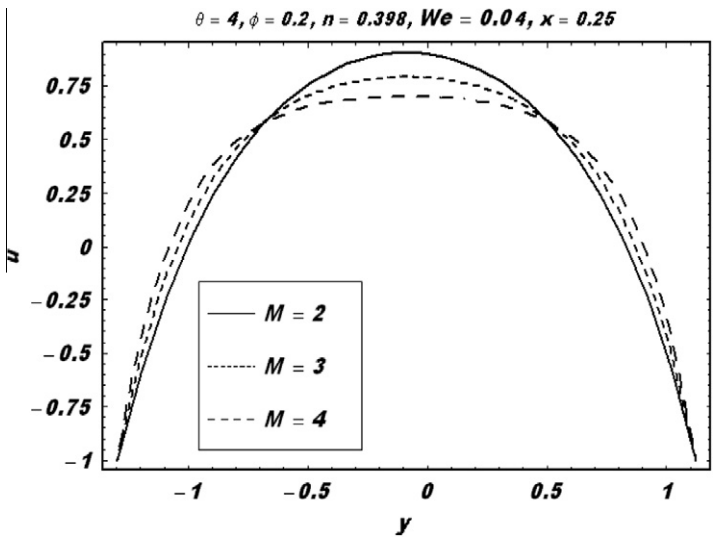

Fig. 15a. Velocity distribution versus y for different values of M.

increases with the decrease of M. In Fig. 2 we have discussed the effects of phase difference (ϕ). It is noticed that in both pumping ($\Delta p_\lambda > 0$) and free ($\Delta p_\lambda = 0$) regions the pumping decreases with an increase of ϕ. However in copumping region ($\Delta p_\lambda < 0$) this situation is quite opposite. The pumping increases for large values of ϕ. It is also noted that pumping rate increases with the decrease of ϕ. Figs. 3 and 4 reveal that pumping rate increases by decreasing the wave amplitudes a and b. To observe the effects of channel width d on Δp_λ we have presented Fig. 5. It shows that pumping decreases when d increases in pumping and free pumping regions. A quite reverse situation is observed in the copumping region where pumping increases with the increase of the channel width.

Figs. 6–11 describe the influence of Hartman number (M), phase difference (ϕ) and volume flow rate (θ) on the axial induced magnetic field and the current density distribution. In Figs. 6–8 it is focused that an axial induced magnetic field h_x decreases by increasing M, ϕ and θ. Moreover h_x is not symmetric about the origin because the phase difference is taken into account. The axial induced magnetic field is in one direction in some part of the region whereas in the other part it is in opposite direction. The current density distribution with y can be seen in Figs. 9–11. Fig. 9 shows that the current density distribution increases near the channel walls when M increases and decreases near the center of the channel. In Fig. 10 we have observed that J_z decreases with an increase of ϕ whereas in the other region the behavior is reverse. In Fig. 11 it is noted that (contrary to Fig. 9) the current density distribution is an increasing function of volume flow rate θ.

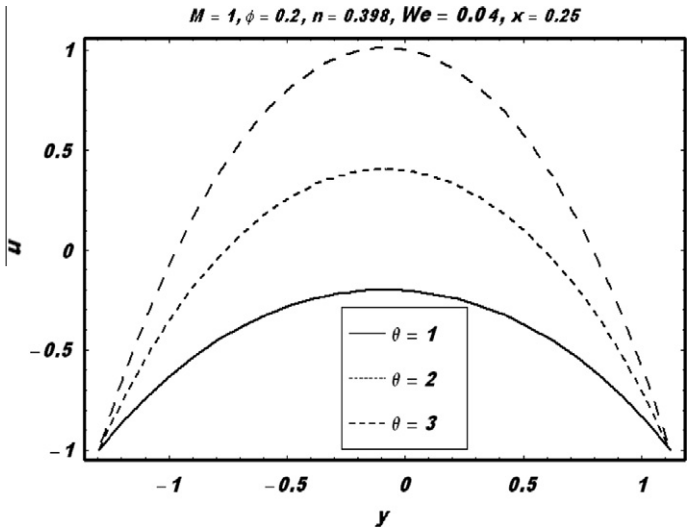

Fig. 15b. Velocity distribution versus y for different values of θ.

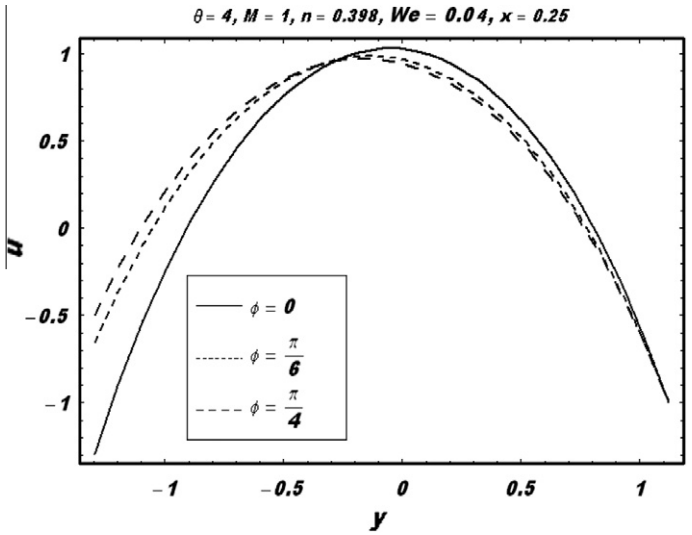

Fig. 15c. Velocity distribution versus y for different values of ϕ.

Figs. 12–14 are for phenomenon of trapping. Figs. 12a and 12b show the streamlines for M. These depicts that size of the trapped bolus decreases with an increase of Hartman number M when $\phi = \frac{\pi}{6}$. Figs. 13a and 13b provide the effects of volume flow rate on trapping. The volume flow rate always affects the trapping phenomenon. These Figures show that the size of bolus increases for large values of θ. Figs. 14a and 14b compare the trapping phenomenon between symmetric and asymmetric channels. This Figure shows that size of the trapped bolus increases by increasing phase difference ϕ. It is also observed that trapped bolus moves towards left for large values of ϕ.

Fig. 15a, 15b and 15c shows the variation of velocity (u) versus y for different parameters. The effect of M on longitudinal velocity (u) at cross section $x = 0.25$ is depicted in Fig. 15a. Here an increase in M causes a decrease in magnitude of u at the boundaries and at the center of the channel u increases for large values of M. In Fig. 15b the effect of θ on u is captured. It is noticed that with an increase in θ the velocity increases. Fig. 15c is just made to see the variation of u for different values of ϕ. It is observed that u increases when ϕ decreases and behavior is quite opposite in the other region. In Figs. 16a, 16b, 16c and 16d we have plotted the temperature distribution (θ') versus y for different values of parameters. In Figs. 16a and 16b θ' increases for large values of Br and for small values of M. Similarly θ' increases with an increase in θ (Fig. 16c). Fig. 16d shows that in the present problem We has no effect on θ'. It is noted from Fig. 16 that the shape of temperature profile is almost parabolic.

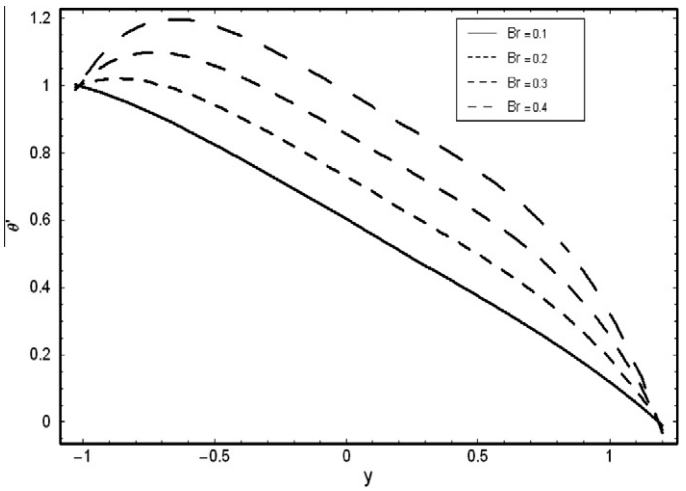

Fig. 16a. Temperature distribution versus y for different values of Br. Here $n = 0.398$, $We = 0.01$, $a = 0.6$, $b = 0.3$, $d = 1.1$, $\epsilon = 0.3$, $M = 1$, $\phi = 0.6$, $\theta = 2$ and $x = 0.2$.

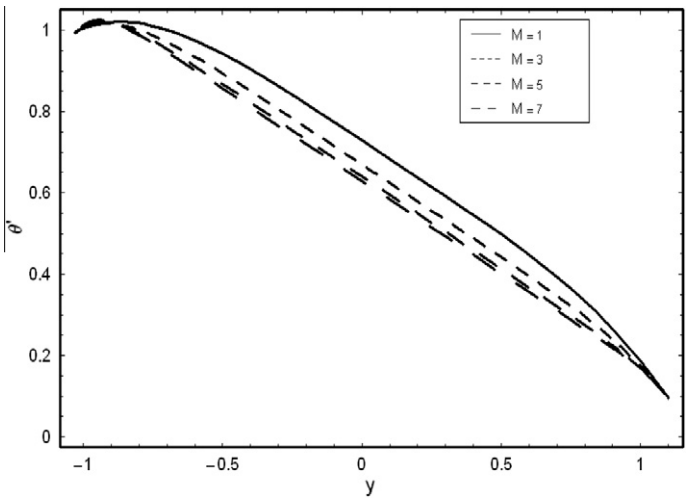

Fig. 16b. Temperature distribution versus y for different values of M. Here $n = 0.398$, $We = 0.01$, $a = 0.6$, $b = 0.3$, $d = 1.1$, $\epsilon = 0.3$, $Br = 0.3$, $\phi = 0.6$, $\theta = 2$ and $x = 0.2$.

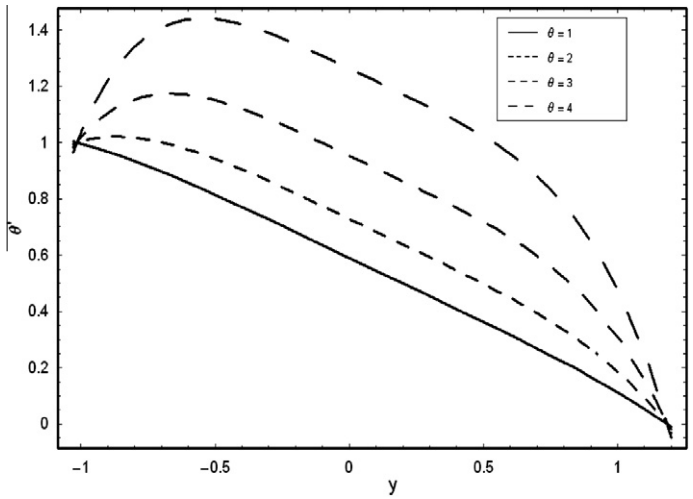

Fig. 16c. Temperature distribution versus y for different values of θ. Here $n = 0.398$, $We = 0.01$, $a = 0.6$, $b = 0.3$, $d = 1.1$, $\epsilon = 0.3$, $Br = 0.3$, $\phi = 0.6$, $M = 1$ and $x = 0.2$.

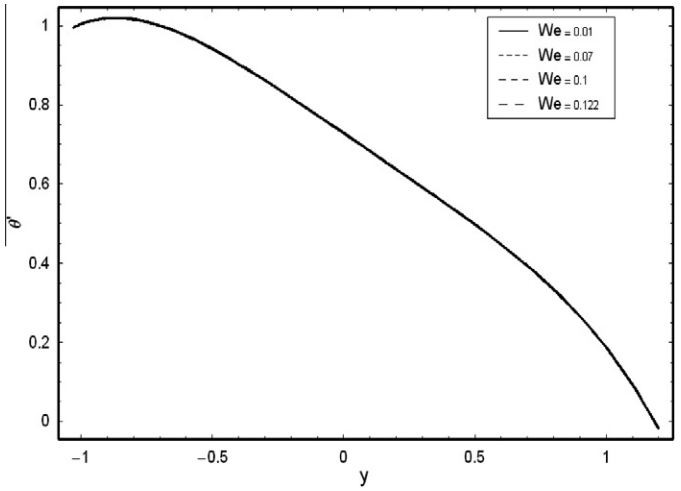

Fig. 16d. Temperature distribution versus y for different values of We. Here $n = 0.398$, $a = 0.6$, $b = 0.3$, $d = 1.1$, $\epsilon = 0.3$, $M = 1$, $Br = 0.3$, $\phi = 0.6$, $\theta = 2$ and $x = 0.2$.

Acknowledgment

The authors gratefully acknowledge the financial support from the Deanship of Scientific Research (DSR) at King Abdulaziz University (KAU) represented by the unit of Research through the grant number (10/31/Gr) for the group entitled Nonlinear Analysis and Applied Mathematics.

References

[1] Latham TW. Fluid motion in peristaltic pumps. M.S. thesis, MIT; 1966.
[2] Shapiro AH, Jaffrin MY, Weinberg SL. Peristaltic pumping with long wavelength and low Reynolds number. J Fluid Mech 1969;37:799–825.
[3] Mekheimer KhS, Abd elmaboud Y. The influence of heat transfer and magnetic field on peristaltic transport of Newtonian fluid in a vertical annulus: application of an endoscope. Phys Lett A 2008;372:1657–65.
[4] Srinivas S, Kothandapani M. The influence of heat and mass transfer on MHD peristaltic flow through a porous space with complaint walls. Appl Math Comput 2009;213:197–208.
[5] Kothandapani M, Srinivas S. Peristaltic transport of a Jeffery fluid under the effect of magnetic field in an asymmetric channel. Int J Non-linear Mech 2008;43:915–24.
[6] Srinivas S, Kothandapani M. Peristaltic transport in an asymmetric channel with heat transfer. Int Commun Heat Mass Transfer 2008;35:514–22.
[7] Vajravelu V, Radhakrishnamacharya G, Radhakrishnamurty V. Peristaltic flow and heat transfer in a vertical porous annulus with long wave approximation. Int J Non-linear Mech 2007;42:754–9.

[8] Kothandapani M, Srinivas S. On the influence of wall properties in the MHD peristaltic transport with heat transfer and porous medium. Phys Lett A 2008;372:4586–91.
[9] Mekheimer KhS, Abd elmaboud Y. Peristaltic flow of a couple stress fluid in an annulus: application of an endoscope. Physica A 2008;387:2403–15.
[10] Wang Y, Hayat T, Ali N, Oberlack M. Magnetohydrodynamic peristaltic motion of a Sisko fluid in a symmetric and asymmetric channel. Physica A 2008;387:347–62.
[11] Hayat T, Mahmood FM, Asghar S. Peristaltic flow of magnetohydrodynamic Johson–Segalman fluid. Non-linear Dynam 2005;40:375–85.
[12] Hayat T, Ali N, Abbas Z. Peristaltic transport of a micropolar fluid in a channel with different wave forms. Phys Lett A 2007;370:331–44.
[13] Ali N, Hussain Q, Hayat T, Asghar S. Slip effects on peristaltic transport of MHD fluid with variable viscosity. Phys Lett A 2008;372:1477–89.
[14] Mekheimer KhS. Peristaltic flow of blood under effect of a magnetic field in a non-uniform channels. Appl Math Comput 2004;153:763–77.
[15] Haroun MH. Nonlinear peristaltic flow of a fourth grade fluid in an inclined asymmetric channel. Comput Mater Sci 2007;39:324–33.
[16] Mekheimer KhS. Peristaltic flow of a magneto-micropolar fluid: effect of induced magnetic field. J Appl Math 2008;2008. 23 p. Article ID 570825.
[17] Mekheimer KhS. Effect of the induced magnetic field on peristaltic flow of a couple stress fluid. Phys Lett A 2008;372:4271–8.
[18] Hayat T, Khan Y, Ali N, Mekheimer KhS. Effect of an induced magnetic field on the peristaltic flow of a third order fluid. Numer Methods Part Diff Equat 2010;26(2):345–66.